CATION EXCHANGE OF 1,2,3-TRIAZOLATE METAL-ORGANIC FRAMEWORKS

by

JEFFREY SHOTA GOMBART

A THESIS

Presented to the Department of Chemistry and Biochemistry
and the Robert D. Clark Honors College
in partial fulfillment of the requirements for the degree of
Bachelor of Arts

June 2023

An Abstract of the Thesis of

Jeffrey Gombart for the degree of Bachelor of Arts
in the Department of Chemistry and Biochemistry to be taken June 2023

Title: Cation Exchange Of 1,2,3-Trizole Metal-Organic Frameworks

Approved: _____*Carl Brozek, Ph.D.*_____
Primary Thesis Advisor

Cation exchange of various metal salts into cadmium triazolate was explored using methods outlined by Dr. Mircea Dincă, modified for a shorter reaction time. Products were structurally analyzed using PXRD analysis. Cation exchange products maintained the cadmium triazolate structure apart from copper. Several other metal salts would destroy the crystal structure at higher concentrations while copper would do the same at low concentrations. Solvent and temperature studies were done on the copper exchange reaction, determining that bulkier solvents can reduce the reaction energy while increasing reaction temperature had similar effects of increasing metal solvent concentration. Both UV-Vis-NIR analysis as well as SEM-EDX data suggests that our exchange reactions were successful with presence of cobalt and copper in their respective exchange reactions as well as changing metal characteristics in our exchange products.

Acknowledgements

I would like to thank Dr. Carl Brozek for providing me with the opportunity to explore my interests in material and inorganic chemistry. I would like to thank Dr. Checkers Marshall for taking me under their wing and providing me with support throughout their time in the Brozek lab. With their guidance I found a project that piqued my interest. I also would like to thank graduate student Audrey Davenport for assisting me wrap up this project and graduate student Liam Twight of the Boettcher lab for assisting with ICP-MS analysis. Finally, I would like to thank all members of the Brozek lab for creating a respectful and professional environment while maintaining a sense of community and friendship.

Table of Contents

Background

Metal-organic frameworks (MOFs) are a class of materials defined as a metal ion bridged by organic linkers and are characterized by their high surface area, low density, and porous nature. MOFs have the highest surface area to volume ratio of all known materials making them of great interest in material science. With several different choices of metals and linkers, almost unlimited combinations can be theorized and synthesized, each with unique properties. These properties can be finely tuned due to not only the diversity of combinations, but also their dynamic bonding nature. In this paper, we study cation exchange, one of the synthetic processes which is utilized to tune these materials.

Having potential applications in gas storage/separation, catalysis, and sensor technology, these materials are favored over traditional porous inorganic materials due to their structural tunability. This directly translates to strong control over the materials properties, allowing for the tuning of pore size, conductivity, structural stability, etc. MOFs can undergo post synthetic exchange (PSE) processes in which metal ions or linkers are exchanged from the synthesized MOF material. These exchange reactions can be performed at room temperature, allowing a MOF to maintain its structure while its chemistry can be changed. Doping MOFs with various transition metal ions can change the magnetic and optical character of the MOF, providing a potential avenue for fine tuning these properties in new materials. This also allows for the formation of materials which cannot be readily synthesized from the ground up. Doped MOFs have been used as precursors to form dilute magnetic semiconductor (DMS) materials. Such dynamic materials show potential application in several different fields, highlighting the importance of understanding their properties.

Metal 1,2,3-triazolate MOFs are characterized by a metal cation octahedrally coordinated by 1,2,3 triazole linkers.
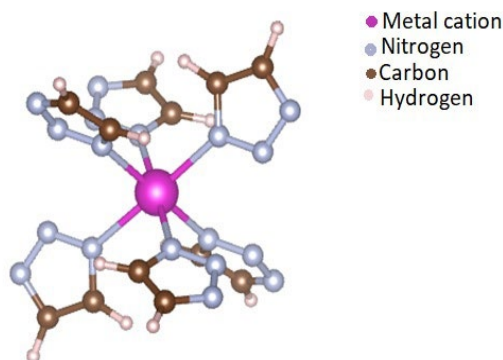

Figure 1: A ball and stick representation of the metal 1,2,3-triazolate MOFs used throughout the project.

The pink atom represents the metal ion within the MOF, while the gray, brown, and tan atoms consist of organic materials (carbon, nitrogen, hydrogen, etc.) and make up the linkers. This figure represents a single cluster of the MOF. The actual MOF product would consist of an array of these clusters with other metal sites binding to available nitrogen atoms on the linkers.

This project focuses on cadmium triazolate (in which cadmium would be the pink cation) and inducing cation exchange to yield a product in which cation impurities exist within the cadmium triazolate material. Cation exchange has become a widely used synthetic process which has unpredictable results. A resulting product could have properties which are the sum of its parts (properties which are relative to the amount of dopant present) or exhibit new properties caused by interactions between the dopant cation and the lattice or the original metal cation. The introduction of dopants can cause the formation of mid-gap orbitals, changing the electronic structure of the material. This allows for fine tuning of MOF semiconductors, necessary for

semiconducting applications. Metal triazolate complexes are one of the few MOFs with semiconducting properties, having potential as a new class of DMS.

Doping the cadmium complex is ideal due to the electronic, optical, and magnetic properties of the metal cation. Being a d10 metal, cadmium has a full set of d-orbital electrons and a relatively stable electronic structure. This causes cadmium-based materials to often be white, as color arises due to these d-d transitions (not possible in d10 elements). A d10 transition metal can be exchanged with a cation which only has partially filled d-orbitals, leading to a product with properties which allow a d-d transitions. This can lead to the development color as well as new photoelectric effects. This also allows for the possibility of a material with magnetic properties, not seen in d10 elements. This can lead to the development of spintronic materials. These materials utilized the additional electron spin degree of freedom along with electronic charge, having the potential to work more efficiently than current technology. DMS act as a bridge between technologies, allowing for electronic control of spintronic devices while still being similar enough to current semiconductor materials to have useful application.

The purpose of these experiments are to verify the effectiveness of the cation exchange method with $Cd(TA)_2$. $Cd(TA)_2$ is a colorless product due to cadmium's electronic properties, allowing for a visible color change with a change in metal character. This provides a visual indicator a cation exchange, making it a good material to perform these experiments. Several different reaction parameters were tested to understand how each effect the product. These products were structurally, optically, elementally analyzed to determine the extent of cation exchange.

Methods

Synthesis

Cadmium Triazolate

Cadmium triazolate was synthesized with methods used by Yaghi and their team. One equivalent of cadmium nitrate tetrahydrate is added to 2.66 equivalents of 1,2,3-triazole in 25 mL of dimethylformamide (DMF). This is put in a Schott bottle and heated in the oven at 120°C for 48 hours. The product is then isolated through centrifugation and washed twice in DMF and once in methanol before dried on a Schlenk line. The resulting product is a colorless white powder.

Cation Exchange

Cation exchange reactions were performed with modified methods used by Dr. Mircea Dincă. Various concentrations of metal salts were dissolved in 10mL methanol are stirred with the $Cd(TA)_2$ in a small reaction vial for 48 hours at room temperature. Cation exchange reactions will be referred to by the equivalents of metal salt used followed by the metal of the salt used (e.g., 40x cobalt reaction). The product was isolated and washed three times with methanol and dried on a Schlenk line.

$$Cd(TA)_2(s) + M_x^+(aq) \xrightarrow{yields} Cd_{1-x}M_x(TA)_2(s)$$
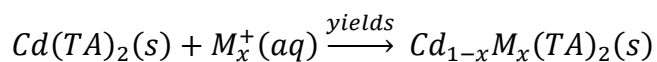
This equation summarizes the cation exchange reactions done for this project. The triazolate linkers are referred to as TA. The cation we want to exchange is denoted as M^+.

Several variables were modified for the cation exchange process including concentration of metal salt used, temperature the reaction was run at, and the solvent used for the exchange

reaction. These variations were done in the attempt to increase product yield and exchange efficiency.

Analysis Techniques

Powder X-Ray Diffraction (PXRD)

PXRD is used to gain structural data on a sample. This is done by hitting a sample with a copper K-α X-ray and measuring the intensity of the diffracted waves. This X-ray interacts with the crystalline planes of the sample, returning peaks which are specific to the structure of the sample. PXRD was run on all samples to determine the crystallinity of the product. Being graphed against a $Cd(TA)_2$ template, we are able to observe if the peaks are aligned confirming the structure of our product. This was done both to confirm the success of our initial $Cd(TA)_2$ product as well as to determine any structural changes in the cation exchange products. We would expect results to show similar crystallinity to our original material, with slight shifts in peaks indicating a changing lattice parameter.

UV-Vis-NIR Diffuse Reflectance Spectroscopy

UV-Vis-NIR scans were performed on dried products to observe changes in optical and electronic behavior. This process involves light waves which reflect off a sample back into a detector, reading the amount light absorbed by or reflected off the sample. The machine scans across several wavelengths from UV to near infrared. Reflectance data was processed using the Kubelka-Munk (K-M) approximations which were normalized using the maximum and minimum values.

$$Km = \frac{(1-R)^2}{2R}$$

This is the equation used to find the K-M transform for a given set of reflectance data. R is the reflectance data normalized.

This was plotted against the energy of the wavelength hitting the sample in eV. From this UV-Vis-NIR data, we can compare how it changes from the parent material to the cation exchange product, looking for the possible d-d transitions which would be otherwise impossible for cadmium. We expect slight changes in UV-Vis-NIR spectrum which indicate metal characteristics of the doped cation, specifically the d-d transitions.

Scanning Electron Microscopy, Energy Dispersive X-Ray Analysis (SEM-EDX)

SEM is an imagine process which allows us to visualize our products at a microscopic scale utilizing beams of electrons to cast the image. This allows us to confirm the crystallinity and get a better estimate of the uniformity of the product. EDX allows chemical characterization and elemental analysis of our product under the scanning electron microscope. When an electron beam from the SEM hits an inner shell electron of an atom, the electron is ejected from the atom creating an electron vacancy. This is then filled by an outer shell electron from the same atom, causing the release of an X-ray with an energy specific to the energy levels of the electron shells. An EDX detector reads the element specific X-ray emissions, mapping their origin on the SEM image. SEM EDX was performed on the cation exchange product to establish if any of the exchanged cation would be present. From our EDX data we expect to see several instances of our doped cation within the material, indicating some level of exchange.

Inductively Coupled Plasma Mass Spectroscopy (ICP-MS)

ICP-MS is an elemental analysis machine used to quantify trace elements or isotopes in a sample. A solid sample must be digested using nitric acid before being passed through the spectrometer which uses an argon plasma torch to ionize each atom. These are sorted by their mass-to-charge ratio and specific ions in the sample are detected and quantified. This is necessary because EDX is not an accurate method of elemental analysis and can only provide a preliminary idea of your sample. ICP-MS provides a much more accurate description of the analyte, necessary for confirming the EDX data. From our ICP-MS data we expect to have a ratio of cadmium cation to doped metal ion present, indicating a successful cation exchange reaction in which the product is doped while maintaining the $Cd(TA)_2$ crystallinity.

Data Processing

PXRD data was visualized with Igor Pro 6 and plotted onto templates with $Cd(TA)_2$ known peaks. PXRD measurements were taken using Bragg-Brentano geometry in the range of 3-40° 2θ with a step size of 0.02°. Products would be put on XRD plates in solution and dried before analysis was performed. UV-Vis-NIR data was worked up in excel using the K-M transform and visualized in Igor Pro 6. Measurements were taken from 3000nm-190nm measuring the percent reflectance. The machine was baselined using $BaSO_4$. Both SEM-EDX and ICP-MS data were provided by the equipment without further processing.

Results and Analysis

Cation exchange experiments were done testing cobalt, copper, iron, manganese, and nickel as exchanging cations. Two cation exchange products showed significant color change. The cobalt exchange product, in which some of the solid would be brown/tan as well as white, and the copper exchange product, which produced a blue solid with low yield and low crystallinity. With cobalt and copper showing promising EDX results, ICPM-S was run only on these samples. Temperature and solvent studies were done for the copper exchange as it was the only cation exchange reaction which would consistently destroy the $Cd(TA)_2$ even at low metal concentrations.
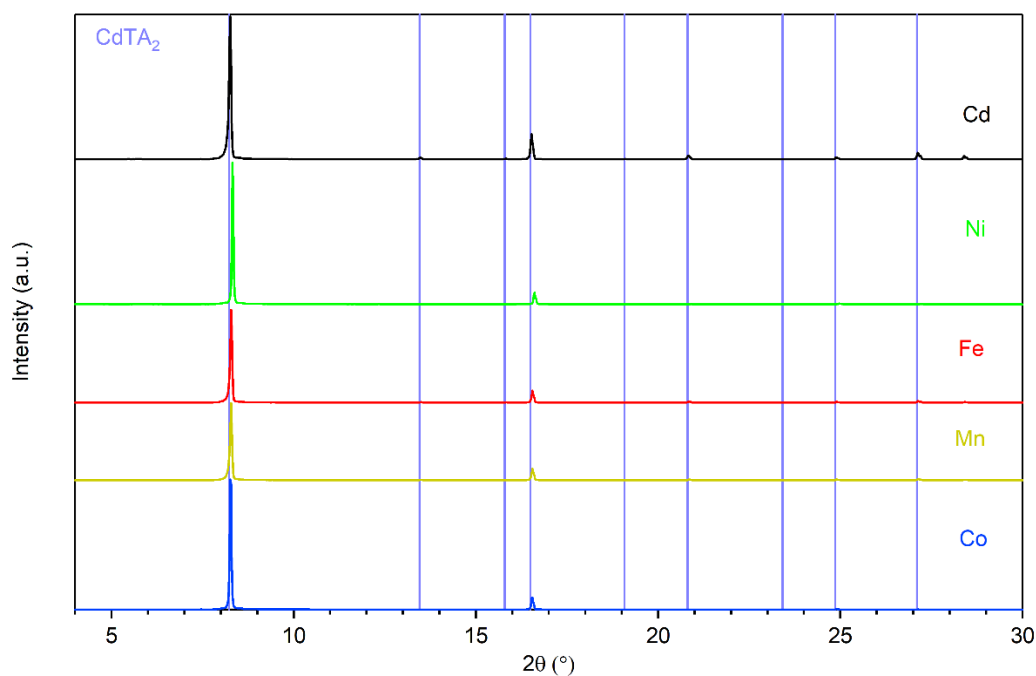

Figure 2: PXRD of cation exchange products.

Reactions were done at metal concentrations 10x that of $Cd(TA)_2$. The metals are color coated to match the data and indicate which metal was exchanged into $Cd(TA)_2$. The pure $Cd(TA)_2$ product is shown at the top, as well as the light blue template which indicate expected peaks for $Cd(TA)_2$.

The peaks which are most prominent are at $2\theta = 8.23$ and 16.50, seen in each of the cation exchange products. Many of the smaller peaks seen in the $Cd(TA)_2$ have been lost but can be seen in the iron exchange product. The presence of the two peaks indicates the crystallinity of the product has not changed drastically. Furthermore, we see a slight shift in the peaks to the right, indicating that the lattice parameter has become slightly smaller. With cadmium having the largest cation radius out of the exchanged metals, this data is consistent with the idea that our metal ions are exchanging into the lattice.

Copper Cation Exchange

When the exchange reaction was done with copper, much of the product would be destroyed, with the remaining solid having a deep blue color. This was peculiar as none of the other reactions would yield significantly less product unless the metal concentration used was extremely high. It was predicted that the exchange was happening too rapidly with copper, causing the process to shred the MOF. Cation exchange of copper was done in butanol, tetrahydrofuran (THF), and DMF rather than methanol. These solvents are bulkier than methanol and were selected to potentially reduce the cation exchange speed. With a bigger solvent, cations would have fewer degrees of freedom and thus slow down the cation exchange.
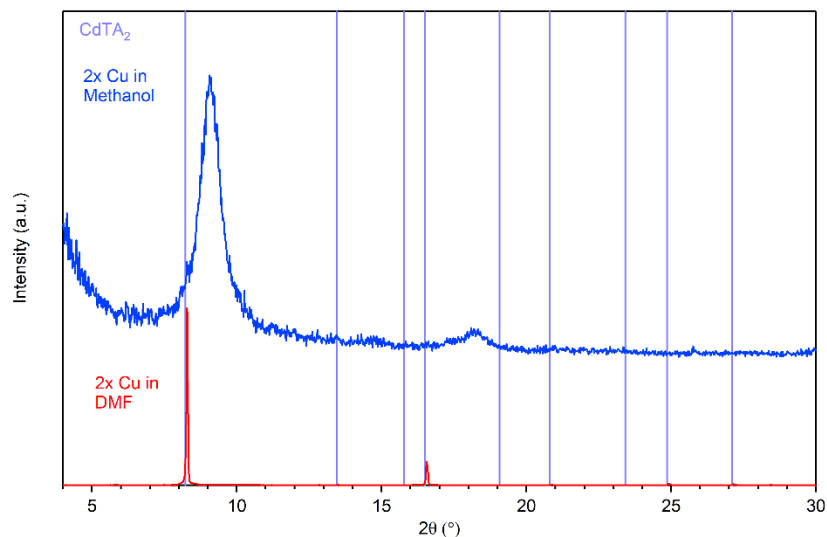
Figure 3: PXRD data of the copper cation exchange reaction in methanol and DMF.

The data for the cation exchange reaction in THF and butanol yielded results like in methanol. The intensity of the methanol peaks was artificially increased to better show the shape of the data. The intensity is too low due to the quality of the product.

The DMF reaction was the only one to yield a substantial amount of product. The same reaction was done at temperatures of 60°C, 80°C, 100°C, and 120°C to observe the effects of increasing cation exchange reaction temperature. Understanding how the reaction temperature affects the product provides another degree of control with the exchange reaction. Increasing temperature had similar effects to increasing metal ion concentration, causing the MOF to break apart in most cases. These parameters would be considered when trying cation exchange with new metal ions.
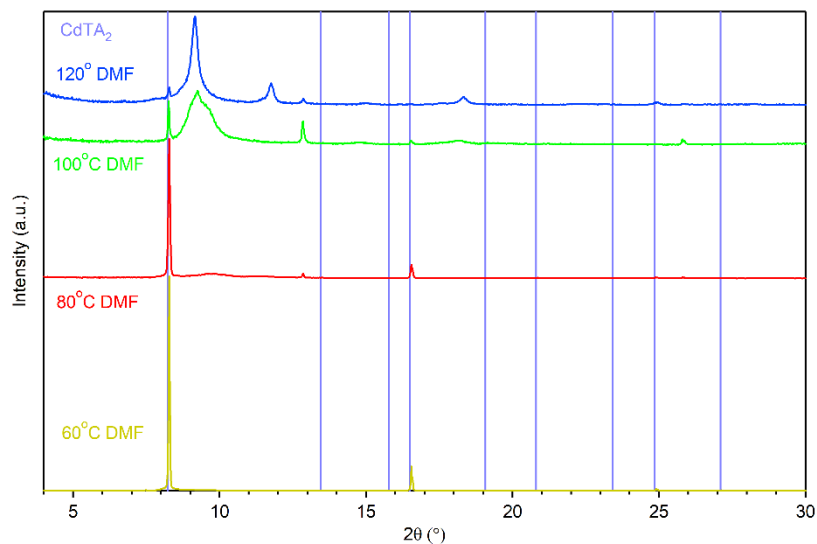
Figure 4: PXRD data of copper cation exchange in DMF.

The intensity of peaks for the 80°C, 100°C, and 120°C products are significantly less than the 60°C reactions.

The higher temperature reactions began breaking apart the MOF as shown by the shrinking peak at $2\theta = 8.23$. We see the formation of new peaks throughout the data, suggesting the formation of some other product. These new peaks look similar to those in the methanol copper exchange, especially the broad peaks around $2\theta = 9$ and 18. Increasing the temperature seemed to have the same effect as increasing the metal concentration in the cation exchange reaction. These reactions are energetically restricted by the strength of the parent MOF as well as the energy necessary for certain cations to replace cadmium.

Low concentration copper exchange (0.1 equivalents Cu with 1equivalent Cd(TA)$_2$) in methanol yielded a similar product to the 60°C DMF exchange reaction and was characterized with UV-Vis-NIR.
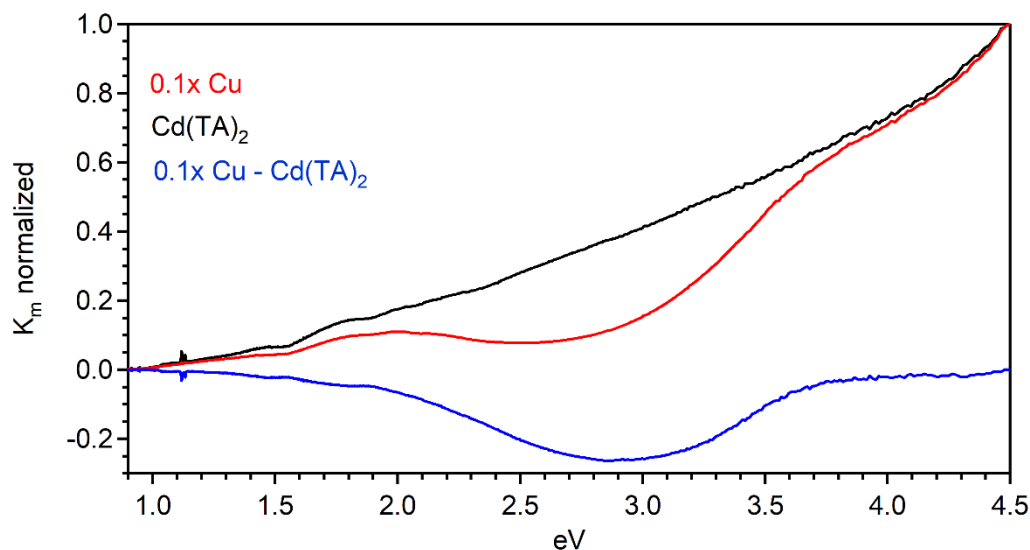
15

Figure 5: UV-Vis-NIR data of the 0.1x Cu exchange product. The data from the exchange product was subtracted from the original $Cd(TA)_2$ (blue) to emphasize peaks only present in our exchange product.

The figure shows a deviation from $Cd(TA)_2$ and the development of a feature around 2-3.5 eV indicating change in metal character. The data was normalized to a range of 4.5 eV to emphasize the changes happening in the range of the d-d transitions.

The development of the feature from 2-3.5 eV indicates a change in metal characteristic, suggesting the presence of copper in our exchanged product. This feature is caused either by d-d transitions occurring in copper in our material or due to a charge transfer in which electron density is redistributed causing an increase in character of the more electronegative complex. With promising UV-Vis-NIR data, SEM-EDX must be run to determine the distribution of our exchange ions.
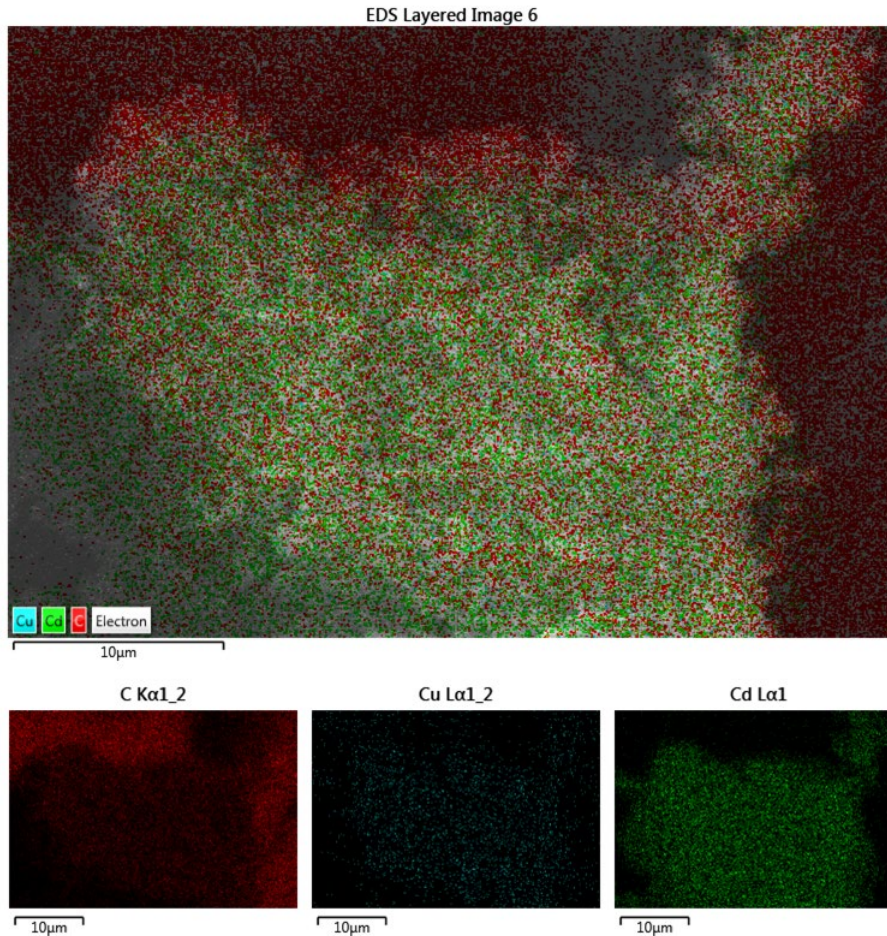
Figure 6: SEM-EDX analysis of the 0.1x Cu exchange product.

This figure shows the EDX mapping of carbon, copper, and cadmium. Carbon makes up the surface the sample was on, explaining the large amount of carbon signal above and to the right of the sample. The top image layers the EDX map onto the actual SEM image taken of the sample.

Figure 6 indicates a significant amount of copper present on the sample surface of our product. EDX detected 5.25% copper by weight with the remaining atoms being cadmium. With data from EDX showing copper in our product.

Cobalt Cation Exchange

The cobalt exchange reaction was of great interest because the product showed a visual color change while maintaining the $Cd(TA)_2$ lattice structure.
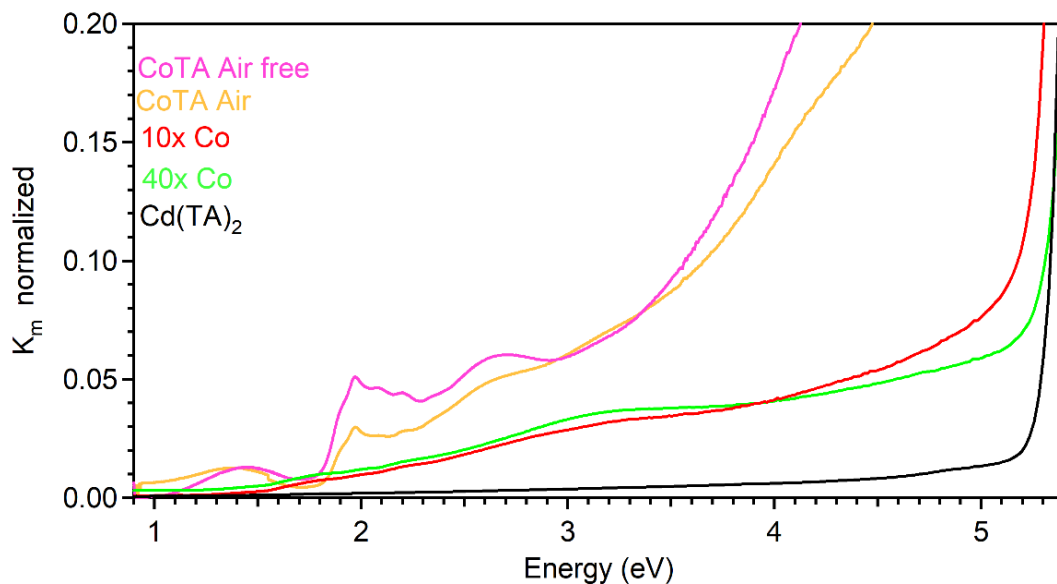
Figure 7: UV-Vis-NIR data of 10x and 40x equivalent cobalt exchanged reaction products.

This figure shows the UV-Vis-NIR data of two cobalt exchange reactions compared with data from Cd(TA)$_2$ and two cobalt triazolate (CoTA) templates (one synthesized in air free conditions).

The d-d transitions in the cobalt triazolate complex are around 1.5-2 eV as seen in the UV-Vis-NIR data of the cobalt triazolate templates. These d-d transitions appear as relatively weak signals with broad peaks. The cation exchange products show an increased reflectance in the 1.7-5 eV, similar to the cobalt triazolate templates.
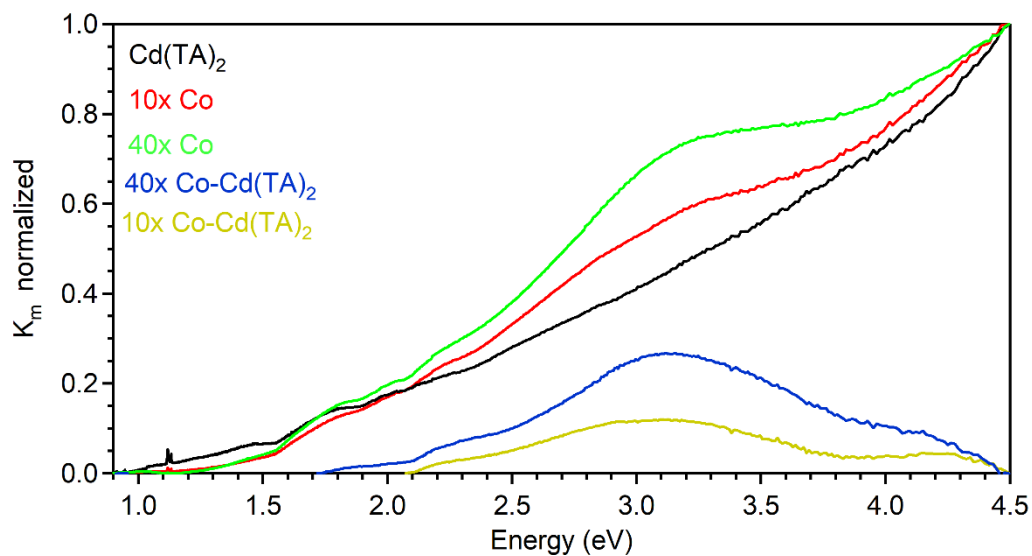
Figure 8: UV-Vis-NIR data of 10x and 40x cobalt exchanges with data from the original Cd(TA)$_2$ material.

This data was normalized to 4.5 eV again to better compare metal characteristics. The Co(TA) templates were removed due to the inability to normalized this data.

We see the development of features from 2-4.5 eV in our cobalt exchange products, indicating a difference in metal character between our cation exchange product and the original material. Similarly, these are likely caused by charge transfer if not d-d transitions arising from the cobalt.
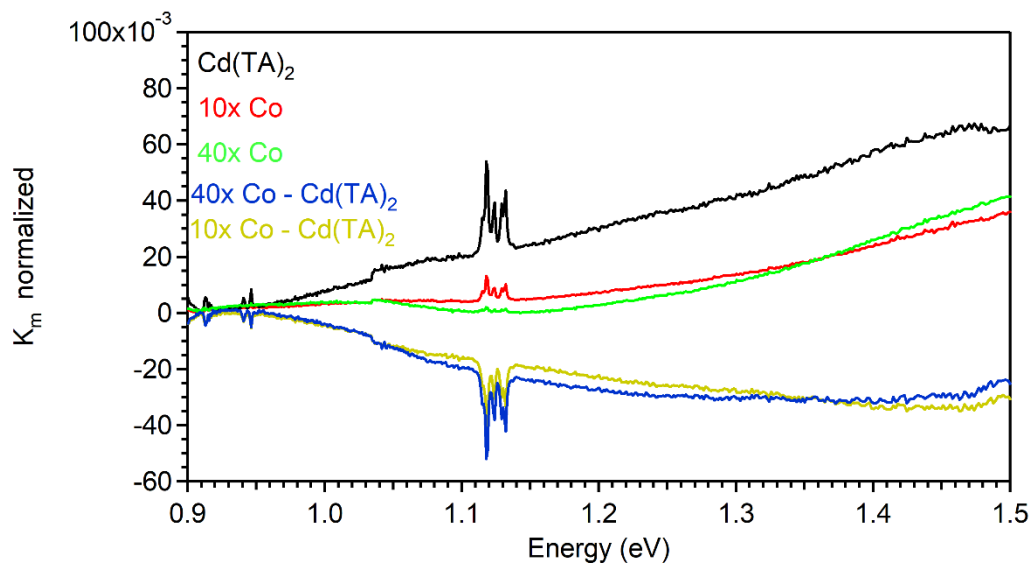
Figure 9: Cobalt exchange UV-Vis-NIR data zoomed to 1-1.5 eV.

This data was graphed to show possible indications of the development of the feature seen at 1-1.5 eV in figure 7 (in the CoTA templates).

However, the feature around 1-1.5 eV was not prominent in our product. There is an indication of a change in UV-Vis-NIR data, but no clear features formed. The product was then analyzed through SEM-EDX analysis to measure the presence of our exchange cation.
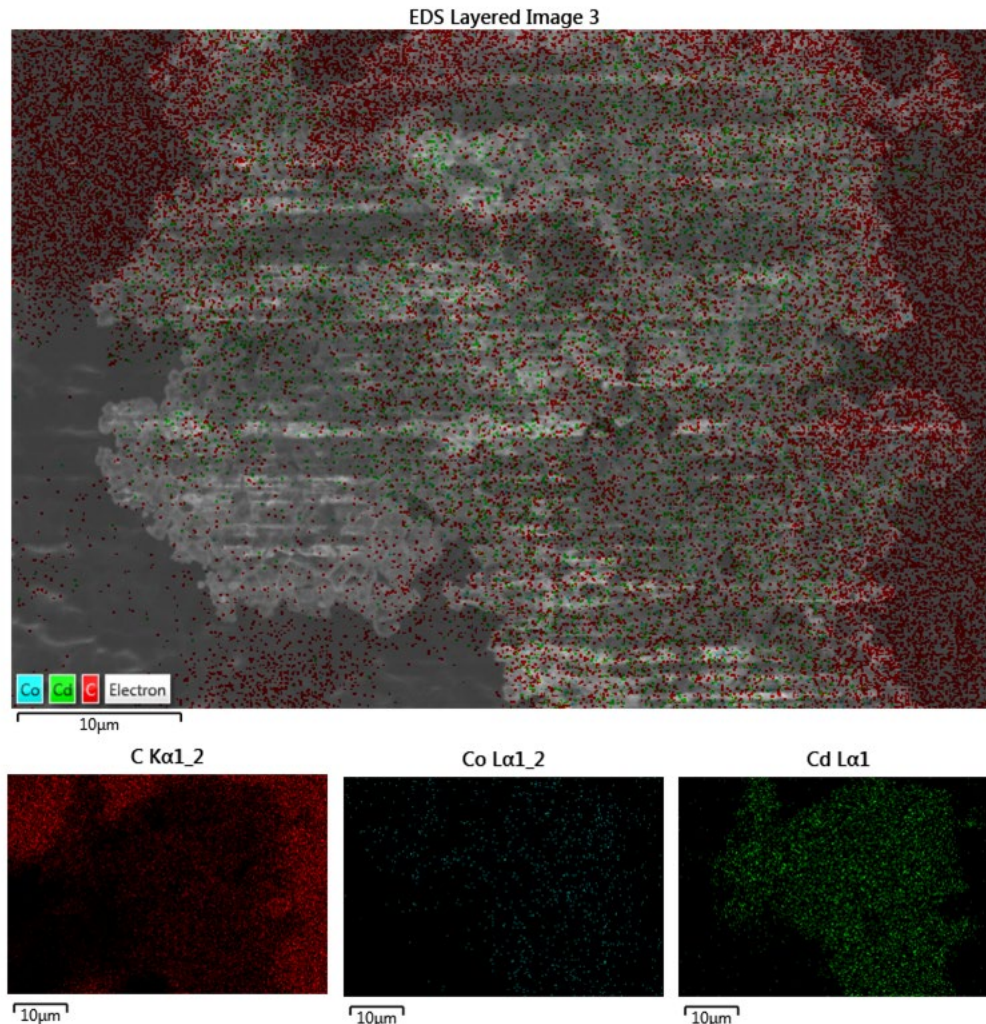
Figure 10: EDX data of the 40x cobalt exchange product.

This figure shows the EDX mapping of cobalt, cadmium, and carbon.

The EDX data shows the presence of cobalt on the surface of our sample. The analysis shows just under 10% of the detected atoms as cobalt with the remaining atoms being cadmium. This level of elemental analysis is not conclusive, however provides enough evidence to run ICP-MS on our cobalt exchange samples.

ICP-MS was not successfully run for either of the cation exchange products. Though we were able to produce calibration curves, our samples would often be too concentrated or contaminated.

Discussion

Figure 2 shows how several different metal salts are potentially able to be incorporated into this MOF using this method of cation exchange. The reaction is able to occur with different cations while maintaining the crystallinity of $Cd(TA)_2$. Furthermore, we see a small shift to the right in the peaks for the cation exchange products.

$$n\lambda = 2dsin\theta$$

> This is the Bragg's law equation that is the basis of XRD analysis in which λ is the wavelength of the X-ray (1.5406 angstrom for copper K-α), d is the lattice spacing, θ is the incident angle of the X-ray, and n is an integer.

Using Bragg's law, we determined that the crystal lattice size (d) has decreased slightly. With cadmium having the largest ionic radius, the peak shifts are consistent with smaller cations exchanging with cadmium.

The copper exchange products show that the identity of the metal being exchanged impacts the kinetics of this reaction. The effects of changing the metal ion concentration or temperature are similar, with increasing metal concentration yielding results identical to increasing reaction temperature. By optimizing reaction conditions, we were able to run the cation exchange reaction with copper without destroying the MOF. With such low concentrations of copper destroying the MOF, it shows that this exchange with copper is highly favorable making it of great interest moving forward. Understanding these effects will provide future experiments with a better understanding of the reaction parameters, allowing for new metals to be potentially exchanged as well as the optimization of previous exchange reactions to yield stronger results.

The cobalt exchange reaction showed a significant color change, indicating a change in metal characteristics. $Cd(TA)_2$ is purely white due to cadmiums full set of d-orbitals so any color

change is only possible with the presence of cobalt. Furthermore, the copper exchange was significant due to the unique reaction results indicating the exchange was happening at a fast rate. UV-Vis-NIR analysis of both exchange products indicated changing metal character with the development of features only possible due to the presence of the exchanged metal.

ICP-MS analysis was inconsistent, with problems arising with both sample concentration as well as sample contamination. Several sets of ICP-MS were performed on cobalt, cooper, and nickel exchange products. Though good calibration curves were produced, most samples would have a concentration too high to definitively make any conclusions about our product. Furthermore, some samples were contaminated, indicating the presence of analytes which could not have been in the sample. Samples would have to be remade with extra precautions as to not cross contaminate samples. This would include properly soaking equipment used to prepare samples and properly storing samples. Though these precautions were taken, ICP-MS is a highly sensitive analysis technique as it separates our samples atomically.

Conclusion/Outlook

Our research lays the foundation for future cation exchange experiments with $Cd(TA)_2$. Data shows this method of cation exchange can be performed on $Cd(TA)_2$ without destroying the MOF structure. This is important because we wish to maintain certain structure specific characteristics while introducing new properties such as magnetism and d-d transitions (color). Both our UV-Vis-NIR and SEM-EDX data show the presence of both cobalt and copper in their respective exchange products, indicating a successful exchange reaction. We need to further optimize the cation exchange reactions through fine tuning parameters discussed in this paper to induce higher rates of cation exchange in our products. Future research should aim to induce color change or significant change in UV-Vis-NIR data. Furthermore, exchange reaction should be done with different metal salts to understand the effects of different elements and to expand our knowledge on the effectiveness and mechanism of reaction.

Bibliography

Allendorf, M. D., Stavila, V., Witman, M., Brozek, C. K., & Hendon, C. H. (2021). What Lies beneath a Metal–Organic Framework Crystal Structure? New Design Principles from Unexpected Behaviors. Journal of the American Chemical Society, 143(18), 6705-6723. https://doi.org/10.1021/jacs.0c10777

Arshadi, M., Amiri, M. J., & Mousavi, S. (2014). Kinetic, equilibrium and thermodynamic investigations of Ni(II), Cd(II), Cu(II) and Co(II) adsorption on barley straw ash. Water Resources and Industry, 6, 1-17. https://doi.org/https://doi.org/10.1016/j.wri.2014.06.001

Brozek, C. K., Bellarosa, L., Soejima, T., Clark, T. V., López, N., & Dincă, M. (2014). Solvent-dependent cation exchange in metal-organic frameworks. Chemistry, 20(23), 6871-6874. https://doi.org/10.1002/chem.201402682

Brozek, C. K., Cozzolino, A. F., Teat, S. J., Chen, Y.-S., & Dincă, M. (2013). Quantification of Site-Specific Cation Exchange in Metal–Organic Frameworks Using Multi-Wavelength Anomalous X-ray Dispersion. Chemistry of Materials, 25(15), 2998-3002. https://doi.org/10.1021/cm400858d

Brozek, C. K., & Dincă, M. (2014). Cation exchange at the secondary building units of metal–organic frameworks. Chem. Soc. Rev., 43(16), 5456-5467. https://doi.org/10.1039/c4cs00002a

Dincă, M., & Long, J. R. (2007). High-Enthalpy Hydrogen Adsorption in Cation-Exchanged Variants of the Microporous Metal−Organic Framework Mn3[(Mn4Cl)3(BTT)8(CH3OH)10]2. Journal of the American Chemical Society, 129(36), 11172-11176. https://doi.org/10.1021/ja072871f

Dodson, R. A., Kalenak, A. P., & Matzger, A. J. (2020). Solvent Choice in Metal–Organic Framework Linker Exchange Permits Microstructural Control. Journal of the American Chemical Society, 142(49), 20806-20813. https://doi.org/10.1021/jacs.0c10224

Gándara, F., Uribe-Romo, F. J., Britt, D. K., Furukawa, H., Lei, L., Cheng, R., Duan, X., O'Keeffe, M., & Yaghi, O. M. (2012). Porous, Conductive Metal-Triazolates and Their Structural Elucidation by the Charge-Flipping Method. Chemistry - A European Journal, 18(34), 10595-10601. https://doi.org/10.1002/chem.201103433

Gao, S., Li, W., Dai, J., Wang, Q., & Suo, Z. (2021). Effect of transition metals doping on electronic structure and optical properties of β-Ga2O3. Materials Research Express, 8(2), 025904. https://doi.org/10.1088/2053-1591/abde10

Huang, Y.-Q., Ding, B., Gao, H.-L., Cheng, P., Liao, D.-Z., Yan, S.-P., & Jiang, Z.-H. (2005). Syntheses, structures and characterization of novel cobalt(II) mono- and bi-triazole complexes. Journal of Molecular Structure, 743(1), 201-207. https://doi.org/https://doi.org/10.1016/j.molstruc.2005.03.010

Khalid, K., Tan, X., Mohd Zaid, H. F., Tao, Y., Lye Chew, C., Chu, D.-T., Lam, M. K., Ho, Y.-C., Lim, J. W., & Chin Wei, L. (2020). Advanced in developmental organic and inorganic nanomaterial: a review. Bioengineered, 11(1), 328-355. https://doi.org/10.1080/21655979.2020.1736240

Kreno, L. E., Leong, K., Farha, O. K., Allendorf, M., Van Duyne, R. P., & Hupp, J. T. (2012). Metal–Organic Framework Materials as Chemical Sensors. Chemical Reviews, 112(2), 1105-1125. https://doi.org/10.1021/cr200324t

Marshall, C. R., Dvorak, J. P., Twight, L. P., Chen, L., Kadota, K., Andreeva, A. B., Overland, A. E., Ericson, T., Cozzolino, A. F., & Brozek, C. K. (2022). Size-Dependent Properties of Solution-Processable Conductive MOF Nanocrystals. Journal of the American Chemical Society, 144(13), 5784-5794. https://doi.org/10.1021/jacs.1c10800

Marshall, C. R., Staudhammer, S. A., & Brozek, C. K. (2019). Size control over metal–organic framework porous nanocrystals. Chemical Science, 10(41), 9396-9408. https://doi.org/10.1039/c9sc03802g

Mínguez Espallargas, G., & Coronado, E. (2018). Magnetic functionalities in MOFs: from the framework to the pore [10.1039/C7CS00653E]. Chemical Society Reviews, 47(2), 533-557. https://doi.org/10.1039/C7CS00653E

Nasi, H., Chiara Di Gregorio, M., Wen, Q., Shimon, L. J. W., Kaplan-Ashiri, I., Bendikov, T., Leitus, G., Kazes, M., Oron, D., Lahav, M., & Van Der Boom, M. E. (2022). Directing the Morphology, Packing, and Properties of Chiral Metal–Organic Frameworks by Cation Exchange**. Angewandte Chemie International Edition, 61(34). https://doi.org/10.1002/anie.202205238

Ruan, C.-Z., Wen, R., Liang, M.-X., Kong, X.-J., Ren, Y.-P., Long, L.-S., Huang, R.-B., & Zheng, L.-S. (2012). Two Triazole-Based Metal–Organic Frameworks Constructed from Nanosized Cu_{20} and Cu_{30} Wheels. Inorganic Chemistry, 51(14), 7587-7591. https://doi.org/10.1021/ic3003299

Santaclara, J. G., Olivos-Suarez, A. I., Gonzalez-Nelson, A., Osadchii, D., Nasalevich, M. A., Van Der Veen, M. A., Kapteijn, F., Sheveleva, A. M., Veber, S. L., Fedin, M. V., Murray, A. T., Hendon, C. H., Walsh, A., & Gascon, J. (2017). Revisiting the Incorporation of Ti(IV) in UiO-type Metal–Organic Frameworks: Metal Exchange versus Grafting and Their Implications on Photocatalysis. Chemistry of Materials, 29(21), 8963-8967. https://doi.org/10.1021/acs.chemmater.7b03320

Schönfeld, F., Meyer, L. V., Mühlbach, F., Zottnick, S. H., & Müller-Buschbaum, K. (2018). Optical isotherms as a fundamental characterization method for gas sensing with luminescent MOFs by comparison of open and dense frameworks. Journal of Materials Chemistry C, 6(10), 2588-2595. https://doi.org/10.1039/c7tc05002j

Sönmez, M. (2001). Synthesis and characterization of copper(II), nickel(II), cadmium(II), cobalt(II) and zinc(II) complexes with 2-Benzoyl-3-hydroxy-1-naphthylamino-3-phenyl-2-propen-1-on. Turkish Journal of Chemistry, 25, 181-185.

Sun, L., Hendon, C. H., Park, S. S., Tulchinsky, Y., Wan, R., Wang, F., Walsh, A., & Dincă, M. (2017). Is iron unique in promoting electrical conductivity in MOFs? [10.1039/C7SC00647K]. *Chemical Science*, *8*(6), 4450-4457. https://doi.org/10.1039/C7SC00647K

Wang, J., Imaz, I., & Maspoch, D. (2022). Metal−Organic Frameworks: Why Make Them Small? Small Structures, 3(1), 2100126. https://doi.org/10.1002/sstr.202100126

Zhou, Y., Yu, F., Su, J., Kurmoo, M., & Zuo, J. L. (2020). Tuning Electrical- and Photo-Conductivity by Cation Exchange within a Redox-Active Tetrathiafulvalene-Based Metal-Organic Framework. Angew Chem Int Ed Engl, 59(42), 18763-18767. https://doi.org/10.1002/anie.202008941